

# Dynamics of a vortex in a trapped Bose-Einstein condensate

Anatoly A. Svidzinsky and Alexander L. Fetter

*Department of Physics, Stanford University, Stanford, CA 94305-4060*

(November 21, 2018)

We consider a large condensate in a rotating anisotropic harmonic trap. Using the method of matched asymptotic expansions, we derive the velocity of an element of vortex line as a function of the local gradient of the trap potential, the line curvature and the angular velocity of the trap rotation. This velocity yields small-amplitude normal modes of the vortex for 2D and 3D condensates. For an axisymmetric trap, the motion of the vortex line is a superposition of plane-polarized standing-wave modes. In a 2D condensate, the planar normal modes are degenerate, and their superposition can result in helical traveling waves, which differs from a 3D condensate. Including the effects of trap rotation allows us to find the angular velocity that makes the vortex locally stable. For a cigar-shape condensate, the vortex curvature makes a significant contribution to the frequency of the lowest unstable normal mode; furthermore, additional modes with negative frequencies appear. As a result, it is considerably more difficult to stabilize a central vortex in a cigar-shape condensate than in a disc-shape one. Normal modes with imaginary frequencies can occur for a nonaxisymmetric condensate (in both 2D and 3D). In connection with recent JILA experiments, we consider the motion of a straight vortex line in a slightly nonspherical condensate. The vortex line changes its orientation in space at the rate proportional to the degree of trap anisotropy and can exhibit periodic recurrences.

## I. INTRODUCTION

The experimental achievement of Bose-Einstein condensation in confined alkali-atom gases [1–3] has stimulated great interest in the generation and observation of vortices in such systems [4–6]. Rotating a totally anisotropic harmonic trap at an angular frequency  $\Omega$  can, in principle, generate vortices; they are energetically stable for  $\Omega > \Omega_c$  [7–10]. There are several other ideas to create vortices in a trapped Bose-Einstein condensate (BEC) [5,11–20]. Vortex formation in BEC was recently observed experimentally [21–25].

In general, a vortex line in a trapped Bose-Einstein condensate is nonstationary. The vortex line can move as a whole, undergo deformation of its shape or perform oscillatory motion like helical waves [26,27]. An extensive literature exists on vortex dynamics in superfluids [28]. The nonlinear Schrödinger equation (Gross-Pitaevskii model) [29–33] has served to study the dynamics and reconnection of vortices, their time evolution, and scattering interactions of superfluid vortex rings. Vortex precession in a nonuniform light beam has recently been observed and discussed in terms of the nonlinear Schrödinger equation [34].

The dynamics of a vortex line in a spatially inhomogeneous two-dimension (2D) condensate was considered in [35,36], while the problem of curvature-driven motion of a vortex line in a homogeneous superfluid in three dimensions (3D) was studied in [37]. A normal mode with negative frequency that corresponds to a vortex precession was found numerically [38] and analytically for a large 3D disk-shape BEC [9], and for a small BEC [39]. The motion of vortex lines and rings in Bose-Einstein condensates in harmonic traps was studied in 2D and 3D by numerical solution of the Gross-Pitaevskii equation [40]. Minimum energy configurations of vortices in a rotating trap were considered in [41].

In a nonrotating trap, the vortex state has a higher energy than the ground-state Bose condensate, so that the vortex is thermodynamically unstable [9]. However, the vortex (with unit circulation quantum) is dynamically stable and can decay only in the presence of dissipation. Dissipative dynamics and the decay time of the vortex state (due to the interaction of the vortex with the thermal cloud) in a trapped Bose-condensed gas are discussed in [42], where the friction coefficient is found to be proportional to the temperature. At temperatures relevant to current experiments, one can neglect dissipation in studying the normal modes of the vortex because the vortex decay rate is much smaller than the frequencies of the normal modes.

In this paper we consider the dynamics of a vortex line in a zero-temperature condensate in the Thomas-Fermi (TF) limit, when the vortex core radius  $\xi \sim d^2/R$  is small compared to the mean oscillator length  $d$  and the mean dimension  $R$  of the condensate [here,  $d = (d_x d_y d_z)^{1/3}$  with  $d_i = \sqrt{\hbar/M\omega_i}$  and trap frequencies  $\omega_i$  ( $i = x, y, z$ )]. We derive a general nonlinear equation for the motion of the vortex that includes the effects of the trap potential, the vortex curvature and the angular velocity of the trap rotation [see Eq. (38) below]. Linearization of this equation around stationary configurations gives rise to the equation for the normal modes of the vortex line. We investigate normal modes of the vortex in 2D and 3D condensates. For a 2D condensate there are solutions in the form of helical

waves. For nonrotating trap some of the solutions have negative eigenfrequencies (these modes are formally unstable); furthermore, in a nonaxisymmetric trap, some solutions can have imaginary eigenfrequencies, implying that a straight central vortex line is unstable with respect to finite self-induced curvature.

In a 3D condensate the spectrum of normal modes becomes discrete. For a vortex near the  $z$  axis, the number of normal modes with negative frequency depends on the aspect ratio  $R_{\perp}/R_z$ . A vortex in a disc-shape condensate ( $R_z < R_{\perp}$ ) has only one mode with negative frequency. However, if we change the aspect ratio to a cigar-shape condensate with  $R_{\perp} < R_z$ , more modes with negative frequency appear. Thus it is more difficult to stabilize a vortex in a cigar-shape condensate rather than in a disc-shape one.

The plan of the paper is the following. In Sec. II we derive a general equation of vortex dynamics using the method of matched asymptotic expansions. In Secs. III and IV, we discuss the normal modes of a vortex line for 2D and 3D condensates. In Sec. V we investigate normal modes with imaginary frequencies that appear for a vortex in a nonaxisymmetric condensate. In the last section we study the motion of a straight vortex line in a slightly nonspherical trap.

## II. GENERAL EQUATION OF THE VORTEX DYNAMICS

Consider a condensate in a nonaxisymmetric trap that rotates with an angular velocity  $\mathbf{\Omega}$ . At zero temperature in a frame rotating with the angular velocity  $\mathbf{\Omega}$ , the trap potential  $V_{\text{tr}}$  is time-independent, and the evolution of the condensate wave function  $\Psi$  is described by the time-dependent Gross-Pitaevskii (GP) equation:

$$\left( -\frac{\hbar^2}{2M}\nabla^2 + V_{\text{tr}} + g|\Psi|^2 - \mu(\mathbf{\Omega}) + i\hbar\mathbf{\Omega} \cdot (\mathbf{r} \times \nabla) \right) \Psi = i\hbar\frac{\partial\Psi}{\partial t}, \quad (1)$$

where  $V_{\text{tr}} = \frac{1}{2}M(\omega_x^2x^2 + \omega_y^2y^2 + \omega_z^2z^2)$  is the external trap potential,  $g = 4\pi\hbar^2a/M > 0$  is the effective interparticle interaction strength, and  $\mu(\mathbf{\Omega})$  is the chemical potential in the rotating frame.

We assume that the condensate contains a  $q$ -fold quantized vortex with the position vector  $\mathbf{r}_0(z, t)$ . In this section we use the *method of matched asymptotic expansions* to determine the vortex velocity as a function of the local gradient of the trap potential  $V_{\text{tr}}$ , the vortex curvature  $k$  and the angular velocity  $\mathbf{\Omega}$ , generalizing the two-dimensional results obtained by Rubinstein and Pismen [35,37] to the case of a three-dimensional rotating potential. The method applies when the external potential does not change significantly on distances comparable with the core size  $|q|\xi \ll R_{\perp}$  (this is the TF limit) and when the curvature is not too large ( $k \ll 1/|q|\xi$ ); it matches the outer asymptotic form of the solution of Eq. (1) in the vortex-core region ( $|\boldsymbol{\rho} - \boldsymbol{\rho}_0| \lesssim |q|\xi$ ) with the short-distance behavior of the solution in the region far from the vortex core ( $|\boldsymbol{\rho} - \boldsymbol{\rho}_0| \gg |q|\xi$ ).

To find the solution in the vortex-core region, one may consider Eq. (1) in a local coordinate frame centered at the point  $\mathbf{r}_0$  of the vortex line that moves with the vortex velocity  $\mathbf{V}$ . In the general case, the vortex line has a curvature  $k$  that depends on the specific element in question. We introduce a local coordinate system  $(x, y, z)$ , so that the  $x$  axis is directed along the vortex normal, the  $y$  axis is along the binormal  $\hat{\mathbf{b}}$  and  $z$  axis is along the tangent  $\hat{\mathbf{t}}$  (see Fig. 1).

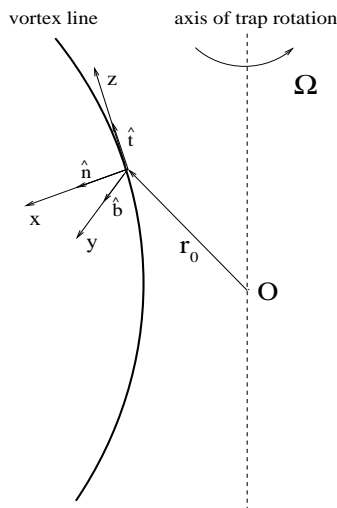


Fig. 1. Local coordinate system associated with the vortex line.

The solution is assumed to be stationary in the comoving frame and satisfies the equation (in the local coordinates):

$$\begin{aligned} \left( -\frac{\hbar^2}{2M} (\nabla^2 - k\partial_x) + V_{\text{tr}}(\mathbf{r}_0) + g|\Psi|^2 - \mu(\Omega) + i\hbar(\boldsymbol{\Omega} \times \mathbf{r}_0) \cdot \nabla \right) \Psi = \\ = -i\hbar \mathbf{V} \cdot \nabla \Psi, \end{aligned} \quad (2)$$

where the term  $-k\partial_x$  arises from the transformation to local coordinates.

One can remove  $\boldsymbol{\Omega}$  from this equation by a shift  $\mathbf{V} \rightarrow \mathbf{V} - (\boldsymbol{\Omega} \times \mathbf{r}_0)$ . In the vortex core region we may seek a solution in the form of an expansion in the small parameters  $\xi/R_\perp$  and  $k\xi$ :

$$\Psi = \Psi_0(\rho) + \Psi_1 = [|\Psi_0(\rho)| - \chi(\rho, z) \cos \phi] e^{iq\phi - i\eta(\rho, z) \sin \phi}, \quad (3)$$

where  $\Psi_0$  is the condensate wave function with  $V_{\text{tr}}$  replaced by  $V_{\text{tr}}(\mathbf{r}_0)$ ; it satisfies a zero-order equation

$$\left( -\frac{\hbar^2}{2M} \nabla^2 + V_{\text{tr}}(\mathbf{r}_0) + g|\Psi_0|^2 - \mu(\Omega) \right) \Psi_0 = 0, \quad (4)$$

and  $\chi, \eta$  characterize the perturbation in the absolute value and phase. Physically  $\Psi_0$  is the analogous wave function for a laterally unbounded condensate with chemical potential  $\mu(\Omega) - V_{\text{tr}}(\mathbf{r}_0)$ . The polar angle  $\phi$  is measured from the direction of the vortex normal ( $\hat{n} \parallel \hat{x}$ ) and  $\rho$  is the radial cylindrical coordinate in the local frame.

The perturbation  $\Psi_1$  obeys the following equation

$$L(\Psi_1, \Psi_1^*) = \frac{2M\hbar}{\hbar} \mathbf{V} \cdot \nabla \Psi_0 + \frac{2M}{\hbar^2} \Psi_0 \boldsymbol{\rho} \cdot \nabla_\perp V_{\text{tr}}(\mathbf{r}_0) + k\partial_x \Psi_0, \quad (5)$$

where

$$L(\Psi_1, \Psi_1^*) \equiv \nabla^2 \Psi_1 + \frac{2M}{\hbar^2} [(\mu(\Omega) - V_{\text{tr}}(\mathbf{r}_0) - 2g|\Psi_0|^2) \Psi_1 - g\Psi_0^2 \Psi_1^*] \quad (6)$$

is a self-conjugate operator and  $\nabla_\perp$  is the gradient operator in a plane perpendicular to the vortex line. This equation is linear in  $\Psi_1$  and in  $\mathbf{V}$ ; it contains  $\nabla_\perp V_{\text{tr}}$  and  $k$  as independent sources, so that the velocity of the vortex line is a sum of independent contributions due to  $\nabla_\perp V_{\text{tr}}$  and  $k$ . Also, the function  $\Psi_0$  depends only on the coordinates in the direction perpendicular to the vortex line; therefore, in the dot product  $\mathbf{V} \cdot \nabla \Psi_0$  only the component of the velocity perpendicular to the vortex line is relevant. We also assume that  $\mathbf{V}$  has no component along the line. For simplicity, one can assume that  $\nabla_\perp V_{\text{tr}}$  lies along  $\hat{n}$  and derive the vortex velocity as a sum of two independent contributions. The final result written in vector form remains valid for arbitrary directions of  $\nabla_\perp V_{\text{tr}}$  and  $\hat{n}$ . Under this assumption, we have  $\mathbf{V} \cdot \nabla \Psi_0 = V \partial_y \Psi_0 = V (\sin \phi \partial_\rho + \rho^{-1} \cos \phi \partial_\phi) \Psi_0$  in polar coordinates. Then, writing  $\Psi_1 = -(\chi \cos \phi + i\eta |\Psi_0| \sin \phi) e^{iq\phi}$  in terms of the small perturbations  $\chi$  and  $\eta$ , Eq. (5) has the form:

$$\begin{aligned} \left( \partial_{\rho\rho}^2 + \frac{1}{\rho} \partial_\rho + \partial_{zz}^2 \right) \chi + \frac{2M}{\hbar^2} (\mu(\Omega) - V_{\text{tr}}(\mathbf{r}_0) - 3g|\Psi_0|^2) \chi - \frac{q^2 + 1}{\rho^2} \chi - \frac{2q}{\rho^2} |\Psi_0| \eta \\ = \frac{2M}{\hbar^2} |\Psi_0| \left( \frac{\hbar q}{\rho} V - \rho |\nabla_\perp V_{\text{tr}}(\mathbf{r}_0)| \right) - k\partial_\rho |\Psi_0| \end{aligned} \quad (7)$$

$$\begin{aligned} \left( \partial_{\rho\rho}^2 + \frac{1}{\rho} \partial_\rho + \partial_{zz}^2 - \frac{1}{\rho^2} \right) \eta + \frac{2}{|\Psi_0|} \left( \partial_\rho |\Psi_0| \partial_\rho \eta + \partial_z |\Psi_0| \partial_z \eta - \frac{q}{\rho^2} \chi \right) \\ = -\frac{2M}{\hbar} V \frac{\partial_\rho |\Psi_0|}{|\Psi_0|} + \frac{kq}{\rho} \end{aligned} \quad (8)$$

We can remove  $V$  from these equations with the following gauge transformation:

$$\eta = \tilde{\eta} - \frac{M}{\hbar} \rho V \quad (9)$$

Further, for large distances  $|q|\xi \ll \rho \ll R_\perp$ , we can use  $g|\Psi_0|^2 \approx g|\Psi_{TF}|^2 \approx \mu(\Omega) - V_{\text{tr}}(\mathbf{r}_0)$  and rewrite Eqs. (7) and (8) as follows

$$2g|\Psi_{TF}|\chi = \rho|\nabla_\perp V_{\text{tr}}(\boldsymbol{\rho}_0)| + \frac{k\hbar^2}{2M|\Psi_{TF}|}\partial_\rho|\Psi_0|, \quad (10)$$

$$\left(\partial_{\rho\rho}^2 + \frac{1}{\rho}\partial_\rho - \frac{1}{\rho^2}\right)\tilde{\eta} - \frac{\chi}{|\Psi_{TF}|}\frac{2q}{\rho^2} = \frac{kq}{\rho}; \quad (11)$$

equivalently,

$$\chi = \frac{\rho}{2g|\Psi_{TF}|}|\nabla_\perp V_{\text{tr}}(\mathbf{r}_0)| + \frac{k\hbar^2}{4Mg|\Psi_{TF}|^2}\partial_\rho|\Psi_0|, \quad (12)$$

$$(\rho^2\partial_{\rho\rho}^2 + \rho\partial_\rho - 1)\tilde{\eta} - \frac{q\rho|\nabla_\perp V_{\text{tr}}(\mathbf{r}_0)|}{g|\Psi_{TF}|^2} = kq\rho + \frac{qk\hbar^2\partial_\rho|\Psi_0|}{2Mg|\Psi_{TF}|^3}. \quad (13)$$

In Eq. (13), we can omit the last term, which is smaller with respect to the term  $kq\rho$  by the factor  $\xi^4/\rho^4$ . As a result, for  $\rho \gg |q|\xi$  the perturbations have the following asymptotic form:

$$\eta \approx \frac{q}{2}\left(\frac{|\nabla_\perp V_{\text{tr}}(\mathbf{r}_0)|}{g|\Psi_{TF}|^2} + k\right)\rho \ln(A\rho) - \frac{M}{\hbar}\rho(\mathbf{V} + \boldsymbol{\Omega} \times \mathbf{r}_0) \cdot \hat{y}, \quad (14)$$

$$\chi \approx \frac{|\nabla_\perp V_{\text{tr}}(\mathbf{r}_0)|}{2g|\Psi_{TF}|}\rho + \frac{k\hbar^2}{4Mg|\Psi_{TF}|^2}\partial_\rho|\Psi_0|. \quad (15)$$

In terms of the phase  $S$ , the solution (14) (the inner expansion in the coordinate frame centered at the vortex line) has the form:

$$S = q\phi - \frac{q}{2}\left(\frac{|\nabla_\perp V_{\text{tr}}(\mathbf{r}_0)|}{g|\Psi_{TF}|^2} + k\right)\ln(A\rho)y + \frac{M}{\hbar}(\mathbf{V} + \boldsymbol{\Omega} \times \mathbf{r}_0) \cdot \mathbf{r} \quad (16)$$

The parameters  $A$  and  $\mathbf{V}$  must be determined by matching the solution (16) with that far from the vortex core.

To the lowest order in the small parameter  $\xi/R_\perp$ , Eq. (1) far from the vortex core reduces to an equation for the condensate phase only

$$|\Psi_{TF}|^2\nabla^2 S + \nabla|\Psi_{TF}|^2 \cdot \nabla S - \frac{M}{\hbar}\boldsymbol{\Omega} \cdot (\mathbf{r} \times \nabla)|\Psi_{TF}|^2 = 0, \quad (17)$$

where  $\Psi = |\Psi|e^{iS}$ . In the frame rotating with the trap and for  $\boldsymbol{\Omega} = \Omega\hat{z}$ , the phase has the form

$$S = S_0 - \frac{M}{\hbar}\frac{(\omega_x^2 - \omega_y^2)}{(\omega_x^2 + \omega_y^2)}\Omega xy, \quad (18)$$

where  $S_0$  is independent of  $\Omega$  [43]. Under a shift of coordinates  $\mathbf{r} \rightarrow \mathbf{r}_0 + \mathbf{r}$ , we have

$$S \approx S_0 + \frac{M}{\hbar}\left((\boldsymbol{\Omega} \times \mathbf{r}_0) + \frac{2}{M(\omega_x^2 + \omega_y^2)}(\nabla V_{\text{tr}}(\mathbf{r}_0) \times \boldsymbol{\Omega})\right) \cdot \mathbf{r}. \quad (19)$$

Comparison of (16) and (19) allows us to find the contribution to the vortex velocity due to the trap rotation

$$\mathbf{V} = \mathbf{V}_0 + \frac{2}{M(\omega_x^2 + \omega_y^2)}(\nabla V_{\text{tr}}(\mathbf{r}_0) \times \boldsymbol{\Omega}), \quad (20)$$

where  $\mathbf{V}_0$  is the velocity for a nonrotating trap.

It is next necessary to find the asymptotic form of  $S_0$  far from the vortex core. This function  $S_0$  satisfies the following equation (in the shifted frame):

$$|\Psi_{TF}|^2 \nabla^2 S_0 + \nabla |\Psi_{TF}|^2 \cdot \nabla S_0 = 0. \quad (21)$$

Introduce a function  $\Phi$  such that

$$S_{0x} = -q (\Phi_y + \Phi \partial_y \ln |\Psi_{TF}|^2), \quad (22)$$

$$S_{0y} = q (\Phi_x + \Phi \partial_x \ln |\Psi_{TF}|^2), \quad (23)$$

where  $S_{0x} = \partial_x S_0$  and  $S_{0y} = \partial_y S_0$ . This representation satisfies Eq. (21) automatically. In addition, the condition

$$\hat{z} \cdot \nabla \times (\nabla_{\perp} S) = S_{0yx} - S_{0xy} = \nabla_{\perp} \cdot (S_{0y} \hat{x} - S_{0x} \hat{y}) = 2\pi q \delta^{(2)}(\rho) \quad (24)$$

gives an equation for  $\Phi$  containing a point source at the vortex location

$$\nabla_{\perp} \cdot [\nabla_{\perp} \Phi + \Phi \nabla_{\perp} \ln |\Psi_{TF}|^2] = 2\pi \delta^{(2)}(\rho). \quad (25)$$

Hence

$$\nabla_{\perp} \cdot \left[ e^{-\ln |\Psi_{TF}|} \nabla_{\perp} (\Phi e^{\ln |\Psi_{TF}|}) - \nabla_{\perp} (e^{-\ln |\Psi_{TF}|}) e^{\ln |\Psi_{TF}|} \Phi \right] = 2\pi \delta^{(2)}(\rho), \quad (26)$$

or

$$e^{-\ln |\Psi_{TF}|} \nabla_{\perp}^2 (\Phi e^{\ln |\Psi_{TF}|}) - \nabla_{\perp}^2 (e^{-\ln |\Psi_{TF}|}) e^{\ln |\Psi_{TF}|} \Phi = 2\pi \delta^{(2)}(\rho). \quad (27)$$

We can put  $\nabla_{\perp}^2 (e^{-\ln |\Psi_{TF}|}) \approx e^{-\ln |\Psi_{TF}|} \nabla_{\perp}^2 V_{\text{tr}} / 2g |\Psi_{TF}|^2$ , so that Eq. (27) becomes

$$\nabla_{\perp}^2 (\Phi e^{\ln |\Psi_{TF}|}) - \frac{\nabla_{\perp}^2 V_{\text{tr}}}{2g |\Psi_{TF}|^2} \Phi e^{\ln |\Psi_{TF}|} = 2\pi \delta^{(2)}(\rho) e^{\ln |\Psi_{TF}|} \quad (28)$$

To find the solution, we rewrite Eq. (28) in the local coordinate frame associated with the vortex line, taking into account the effect of curvature:

$$(\nabla_{\perp}^2 - k \partial_x) (\Phi e^{\ln |\Psi_{TF}|}) - \frac{\nabla_{\perp}^2 V_{\text{tr}}}{2g |\Psi_{TF}|^2} \Phi e^{\ln |\Psi_{TF}|} = 2\pi \delta^{(2)}(\rho) e^{\ln |\Psi_{TF}|}, \quad (29)$$

or

$$\nabla_{\perp}^2 (\Phi e^{\ln |\Psi_{TF}| - kx/2}) - \left( \frac{\nabla_{\perp}^2 V_{\text{tr}}}{2g |\Psi_{TF}|^2} + \frac{k^2}{4} \right) \Phi e^{\ln |\Psi_{TF}| - kx/2} = 2\pi \delta^{(2)}(\rho) e^{\ln |\Psi_{TF}|}. \quad (30)$$

The solution of this inhomogeneous equation is (note that an additional solution of the homogeneous equation does not satisfy the boundary conditions at large  $\rho$  and should be omitted):

$$\Phi = -e^{kx/2} K_0 \left( \sqrt{\frac{\nabla_{\perp}^2 V_{\text{tr}}}{2g |\Psi_{TF}|^2} + \frac{k^2}{4}} \rho \right), \quad (31)$$

where  $K_0$  is a modified Bessel function [for small  $x$ , we have  $K_0 \approx -\ln(e^C x/2)$  where  $C = 0.577\dots$  is the Euler constant]. Further, under the logarithm we may put  $\nabla_{\perp}^2 V_{\text{tr}} / 4g |\Psi_{TF}|^2 \approx 1/R_{\perp}^2$ . Hence  $\Phi$  (in the local coordinate frame centered at the vortex line) has the short-distance form

$$\Phi \approx \ln \left( \frac{e^C}{\sqrt{2}} \sqrt{\frac{1}{R_{\perp}^2} + \frac{k^2}{8}} \rho \right). \quad (32)$$

To make the asymptotic matching, we can express the solution (16) in the vortex-core region in terms of  $\Phi$  and then compare with the formula (32). Using the definitions (22), (23) of the function  $\Phi$ , one can show that the expression (16) (for  $\Omega = 0$ ) corresponds to the following function  $\Phi$  (in the coordinate frame centered at the vortex line):

$$\Phi \approx \left[ 1 + \frac{x}{2} \left( \frac{|\nabla_{\perp} V_{\text{tr}}(\mathbf{r}_0)|}{g |\Psi_{TF}|^2} + k \right) \right] \ln(A\rho) + \frac{MV_0}{\hbar q} x. \quad (33)$$

To verify this expression, we use  $\partial_x \ln |\Psi_{TF}|^2 \approx -|\nabla_{\perp} V_{\text{tr}}(\mathbf{r}_0)|/g|\Psi_{TF}|^2$  and  $\partial_y \ln |\Psi_{TF}|^2 \approx 0$  in the local coordinate frame where  $\Phi_x \rightarrow (\partial_x - k)\Phi$ . Substituting (33) into (22) and (23), we obtain

$$S_{0x} = -\frac{qy}{\rho^2}, \quad (34)$$

$$S_{0y} = \frac{qx}{\rho^2} - \frac{q}{2} \left( \frac{|\nabla_{\perp} V_{\text{tr}}(\mathbf{r}_0)|}{g|\Psi_{TF}|^2} + k \right) \ln(A\rho) + \frac{MV_0}{\hbar}. \quad (35)$$

Therefore, in the coordinate frame centered at the vortex line, the remaining contribution to the phase is

$$S_0 = q\phi - \frac{q}{2} \left( \frac{|\nabla_{\perp} V_{\text{tr}}(\mathbf{r}_0)|}{g|\Psi_{TF}|^2} + k \right) \ln(A\rho) \rho \sin \phi + \frac{M}{\hbar} V_0 \rho \sin \phi \quad (36)$$

which coincides with (16) (for  $\Omega = 0$ ). Matching (33) and (32) (at  $\rho \sim |q|\xi$ ) gives an expression for the constant  $A$  (with logarithmic accuracy):

$$\ln(Ae) = \ln \sqrt{\frac{1}{R_{\perp}^2} + \frac{k^2}{8}}, \quad (37)$$

where  $R_{\perp}$  is the mean transverse dimension of the condensate, and for the velocity  $V_0$ .

Finally, in general vector form (in the frame rotating with the trap), the vortex velocity is:

$$\mathbf{V}(\mathbf{r}_0) = -\frac{q\hbar}{2M} \left( \frac{\hat{t} \times \nabla V_{\text{tr}}(\mathbf{r}_0)}{g|\Psi_{TF}|^2} + k\hat{b} \right) \ln \left( |q|\xi \sqrt{\frac{1}{R_{\perp}^2} + \frac{k^2}{8}} \right) + \frac{2(\nabla V_{\text{tr}}(\mathbf{r}_0) \times \boldsymbol{\Omega})}{\Delta_{\perp} V_{\text{tr}}(\mathbf{r}_0)}, \quad (38)$$

where  $\hat{b}$  is a unit vector in the direction to the vortex binormal,  $\hat{t}$  is a tangent vector to the vortex line and  $\Delta_{\perp}$  is the Laplacian operator in the plane perpendicular to  $\boldsymbol{\Omega}$ . This formula is valid for arbitrary directions of the local gradient of the trap potential, the normal to the vortex line and  $\boldsymbol{\Omega}$ . Near the condensate boundary the denominator of the first term in this formula goes to zero. Therefore,  $\hat{t} \times \nabla V_{\text{tr}}$  must also vanish near the boundary, implying that  $\hat{t}$  is parallel to  $\nabla V_{\text{tr}}$ ; as a result, the vortex line obeys the boundary condition that its axis is perpendicular to the boundary.

### III. NORMAL MODES IN TWO DIMENSIONS

To understand the implications of Eq. (38), it is valuable to consider first the case of a 2D condensate with  $\boldsymbol{\Omega} = \Omega \hat{z}$  and  $\omega_z = 0$  (hence no confinement in the  $z$  direction). Let the vector  $\boldsymbol{\rho}_0(z, t) = (x(z, t), y(z, t))$  describe the time-dependent position of the vortex line during its motion, and  $\mathbf{k}$  be the vector of the principal curvature; then  $k\hat{b} = \hat{t} \times \mathbf{k}$  and  $d^2 \boldsymbol{\rho}_0/ds^2 = \mathbf{k}$ , where  $s$  is the length measured along the vortex line. For small displacements of the line from the  $z$  axis, we have  $s \approx z$ ,  $\hat{t} \approx \hat{z}$  and  $\mathbf{k} \approx d^2 \boldsymbol{\rho}_0/dz^2$ . Then using

$$\hat{z} \times \nabla V_{\text{tr}} = -M\omega_y^2 y \hat{x} + M\omega_x^2 x \hat{y} \quad (39)$$

and

$$k\hat{b} = \hat{t} \times \mathbf{k} \approx -\hat{x} \frac{\partial^2 y}{\partial z^2} + \hat{y} \frac{\partial^2 x}{\partial z^2}, \quad (40)$$

we obtain the following coupled differential equations for  $x(z, t)$  and  $y(z, t)$

$$\frac{\partial x}{\partial t} = \frac{q\hbar}{2M} \left( \frac{2y}{R_y^2} + \frac{\partial^2 y}{\partial z^2} \right) \ln \left( |q|\xi \sqrt{\frac{1}{R_{\perp}^2} + \frac{k^2}{8}} \right) + \frac{4\Omega\mu}{M(\omega_x^2 + \omega_y^2)} \frac{y}{R_y^2}, \quad (41)$$

$$\frac{\partial y}{\partial t} = -\frac{q\hbar}{2M} \left( \frac{2x}{R_x^2} + \frac{\partial^2 x}{\partial z^2} \right) \ln \left( |q|\xi \sqrt{\frac{1}{R_{\perp}^2} + \frac{k^2}{8}} \right) - \frac{4\Omega\mu}{M(\omega_x^2 + \omega_y^2)} \frac{x}{R_x^2}. \quad (42)$$

These equations have solutions in the form of helical waves

$$x = \varepsilon_x \sin(\omega t + \kappa z + \varphi_0), \quad y = \varepsilon_y \cos(\omega t + \kappa z + \varphi_0), \quad (43)$$

with the following dispersion relation between  $\omega$  and  $\kappa$  (under the logarithm we take  $k \approx |\kappa|$ ):

$$\omega = \pm \frac{q\hbar}{2MR_xR_y} \sqrt{(2 - \kappa^2 R_x^2 - \tilde{\Omega})(2 - \kappa^2 R_y^2 - \tilde{\Omega})} \ln \left( |q|\xi \sqrt{\frac{1}{R_\perp^2} + \frac{|\kappa|^2}{8}} \right). \quad (44)$$

The associated amplitudes obey the relation

$$\varepsilon_y = \pm \frac{R_y}{R_x} \varepsilon_x \sqrt{\frac{2 - \kappa^2 R_x^2 - \tilde{\Omega}}{2 - \kappa^2 R_y^2 - \tilde{\Omega}}}, \quad (45)$$

where

$$\tilde{\Omega} = \frac{4MR_x^2R_y^2\Omega}{q\hbar(R_x^2 + R_y^2) \ln \left( |q|\xi \sqrt{\frac{1}{R_\perp^2} + \frac{|\kappa|^2}{8}} \right)^{-1}}, \quad (46)$$

is a dimensionless rotation speed.

For a nonaxisymmetric trap (for example,  $R_x > R_y$ ) the oscillation frequency becomes imaginary if  $\sqrt{(2 - \tilde{\Omega})}/R_x < |\kappa| < \sqrt{(2 - \tilde{\Omega})}/R_y$ , in which case the initial orientation of the vortex line along the  $z$  axis is unstable with respect to the formation of finite curvature. For  $\tilde{\Omega} > \tilde{\Omega}_m = 2$ , however, the oscillation frequency is real (and positive) for any  $\kappa$ . Thus the trap rotation stabilizes a vortex line that initially lies along the  $z$  axis.

For a straight vortex line ( $\kappa = 0$ ), the frequency is always real. This unstable normal mode has the most negative frequency [we choose the sign in (44) that corresponds to positive-norm solution] with

$$\omega = -\frac{q\hbar}{MR_xR_y} \left( \ln \left( \frac{R_\perp}{|q|\xi} \right) - \frac{4\mu\Omega}{q\hbar(\omega_x^2 + \omega_y^2)} \right). \quad (47)$$

For  $q > 0$  and  $\Omega = 0$ , the vortex moves (around the  $z$  axis) counterclockwise in the positive sense. With increasing rotation frequency  $\Omega$  of the trap, the vortex velocity (as seen in the rotating frame) decreases towards zero and vanishes at  $\Omega = \Omega_m$ , where the metastable angular velocity  $\Omega_m$  of trap rotation is given by

$$\Omega_m = \frac{|q|\hbar(\omega_x^2 + \omega_y^2)}{4\mu} \ln \left( \frac{R_\perp}{|q|\xi} \right). \quad (48)$$

This value  $\Omega_m$  corresponds to the angular velocity of trap rotation at which a straight vortex line at the trap center first becomes a local minimum of energy (for  $\Omega < \Omega_m$ , the central position is a local maximum) [9]. For  $\Omega > \Omega_m$  the apparent motion of the vortex becomes clockwise. For  $\kappa = 0$ , this straight vortex follows an elliptic trajectory along the line  $V_{\text{tr}} = \text{const}$ , as expected from the dissipationless character of the GP equation.

For a uniform condensate ( $R_x, R_y \rightarrow \infty$ ), Eq. (44) coincides with the well-known dispersion law of small oscillations of a straight vortex line (Kelvin modes):

$$\omega = \pm \frac{q\hbar}{2M} k^2 \ln(|q|\xi k). \quad (49)$$

Note that one can represent the helical wave solution (43) as a sum of two plane-wave solutions:

$$x_1 = \varepsilon_x \cos(kz) \sin(\omega t + \varphi_0), \quad y_1 = \varepsilon_y \cos(kz) \cos(\omega t + \varphi_0), \quad (50)$$

$$x_2 = \varepsilon_x \sin(kz) \sin(\omega t + \varphi_0 + \pi/2), \quad y_2 = \varepsilon_y \sin(kz) \cos(\omega t + \varphi_0 + \pi/2). \quad (51)$$

One can easily see that Eqs. (50) and (51) are indeed solutions of Eqs. (41) and (42) with the same dispersion law  $\omega = \omega(k)$  as the helical wave (44). In fact, the general motion of the vortex line can be represented as a combination of plane-wave solutions; helical waves are just one of the possible combinations and hence do not represent a different set of solutions. Solutions (50), (51) have different parity, but the same eigenfrequency (in 2D there is degeneracy). In 3D case, the plane-wave solutions are not degenerate and, therefore, in 3D it is impossible to construct a simple analog of helical waves. The general vortex motion in 3D is a combination of plane waves (plane-wave solutions in 3D exist, at least, for an axisymmetric trap) with different numbers of nodes along the symmetry axis and hence different frequencies.

#### IV. DYNAMICS OF A VORTEX IN THREE DIMENSIONS

Let us consider small displacements of the vortex from the  $z$  axis and  $\mathbf{\Omega} = \Omega \hat{z}$ . The vortex curvature is proportional to the vortex displacement, so one can put  $k \approx 0$  under the logarithm in (38). Further, for small displacements

$$\hat{t} \times \nabla V_{\text{tr}} \approx M \left( \hat{x} (\omega_z^2 z y' - \omega_y^2 y) + \hat{y} (\omega_x^2 x - \omega_z^2 z x') \right), \quad (52)$$

where a prime denotes derivative with respect to  $z$ . Then in dimensionless coordinates  $x \rightarrow R_x x$ ,  $y \rightarrow R_y y$ ,  $z \rightarrow R_z z$ , Eq. (38) becomes:

$$\dot{x} = \frac{q\hbar}{2MR_x R_y} \left( \frac{2(\beta z y' - y)}{(1-z^2)} - \beta y'' \right) \ln \left( \frac{R_{\perp}}{|q|\xi} \right) + \frac{4\Omega\mu}{M(\omega_x^2 + \omega_y^2)} \frac{y}{R_x R_y}, \quad (53)$$

$$\dot{y} = -\frac{q\hbar}{2MR_x R_y} \left( \frac{2(\alpha z x' - x)}{(1-z^2)} - \alpha x'' \right) \ln \left( \frac{R_{\perp}}{|q|\xi} \right) - \frac{4\Omega\mu}{M(\omega_x^2 + \omega_y^2)} \frac{x}{R_x R_y}, \quad (54)$$

where

$$\alpha = \frac{R_x^2}{R_z^2}, \quad \beta = \frac{R_y^2}{R_z^2}$$

are parameters characterizing the trap anisotropy. One can seek solution of these equations in the form

$$x = x(z) \sin(\omega t + \varphi_0), \quad y = y(z) \cos(\omega t + \varphi_0)$$

and obtain the following ordinary differential equations for  $x(z)$ ,  $y(z)$  and  $\omega$

$$\tilde{\omega} x = \frac{2(\beta z y' - y)}{(1-z^2)} - \beta y'' + \tilde{\Omega} y, \quad (55)$$

$$\tilde{\omega} y = \frac{2(\alpha z x' - x)}{(1-z^2)} - \alpha x'' + \tilde{\Omega} x, \quad (56)$$

where we introduce dimensionless angular velocities

$$\tilde{\omega} = \frac{2MR_x R_y \omega}{q\hbar \ln \left( \frac{R_{\perp}}{|q|\xi} \right)}, \quad \tilde{\Omega} = \frac{4MR_x^2 R_y^2 \Omega}{q\hbar (R_x^2 + R_y^2) \ln \left( \frac{R_{\perp}}{|q|\xi} \right)}$$

##### A. Stationary configurations

Consider a nonrotating trap with  $\tilde{\Omega} = 0$ . In this section, we seek stationary configurations in which the vortex line remains at rest (in this case, the contributions to the velocity from the vortex curvature and the trap potential compensate each other). To find the stationary configurations we need to solve Eqs. (55) and (56) with the condition  $\tilde{\omega} = 0$ . The resulting equations for  $x$  and  $y$  uncouple; for example, the equation for  $x(z)$  has the form:

$$(1-z^2) x'' - 2zx' + \frac{2}{\alpha} x = 0. \quad (57)$$

The general solution of Eq. (57) can be expressed in terms of hypergeometric functions, but it is impossible to satisfy the boundary conditions that  $x(z)$  should be finite at  $z = \pm 1$  unless  $2/\alpha = n(n+1)$ , where  $n$  is an integer ( $n \geq 0$ ). In this case, the solutions reduce to Legendre polynomials

$$x \propto P_n(z). \quad (58)$$



For example, the first three physical solutions are (we ignore  $n = 0$  which corresponds to  $\alpha = \infty$ ):

$$x_1 = Cz, \quad \alpha = 1 \quad (59)$$

$$x_2 = \varepsilon(1 - 3z^2), \quad \alpha = \frac{1}{3} \quad (60)$$

$$x_3 = C \left( z - \frac{5}{3}z^3 \right), \quad \alpha = \frac{1}{6} \quad (61)$$

If  $2/\alpha \neq n(n+1)$ , the only possible solution of Eq. (57) is the trivial one with  $x = 0$ . The equation for the  $y$  coordinate has the same solutions  $y \propto P_m(z)$ , if  $2/\beta = m(m+1)$ , and  $y = 0$ , if  $2/\beta \neq m(m+1)$ . That is, if  $2/\alpha \neq n(n+1)$  and  $2/\beta \neq m(m+1)$ , there are no stationary configurations of the vortex line apart from the straight orientation along the  $z$  axis.

One should note that the integer  $n$  (or  $m$ ) enumerates the solutions not only for  $\tilde{\omega} = 0$ ; in particular,  $n$  represents to number of times that the vortex line (precessing with angular velocity  $\tilde{\omega}_n$ ) crosses  $z$  axis. For an axisymmetric trap ( $\alpha = \beta$ ), we can consider  $\tilde{\omega}_n$  as a function of  $\alpha$ ; the function  $\tilde{\omega}_n$  changes sign at  $\alpha = \alpha_n = 2/n(n+1)$ . This observation allows us to find the number of normal modes with negative frequency at a fixed value of anisotropy parameter  $\alpha$ . If  $\alpha > 1$  there is only one mode with negative frequency. If  $\frac{1}{3} < \alpha < 1$  there are 2 such normal modes. If  $\frac{1}{6} < \alpha < \frac{1}{3}$  there are 3 modes, and so on. If  $\alpha_n < \alpha < \alpha_{n-1}$  there are  $n$  normal modes with negative frequency.

### B. Dynamics of a vortex in a disk-shape condensate $R_z \ll R_\perp$ : Investigation of unstable mode

In the limit  $\alpha, \beta \gg 1$  the approximate solution of Eqs. (55) and (56) that corresponds to the unstable mode is

$$x = \varepsilon \left( 1 + \frac{z^2}{2\alpha} \right), \quad (62)$$

$$y = \varepsilon \left( 1 + \frac{z^2}{2\beta} \right), \quad (63)$$

with the corresponding eigenvalue

$$\tilde{\omega} = \tilde{\Omega} - 3 - \frac{1}{10} \left( \frac{1}{\alpha} + \frac{1}{\beta} \right). \quad (64)$$

For  $\tilde{\Omega} = 0$  the excitation energy is negative and hence formally unstable. If the trap rotates, the solution (64) becomes stable at  $|\Omega| \geq \Omega_m$ , where

$$\Omega_m = \frac{|q|\hbar(\omega_x^2 + \omega_y^2)}{8\mu} \left( 3 + \frac{1}{10} \left( \frac{1}{\alpha} + \frac{1}{\beta} \right) \right) \ln \left( \frac{R_\perp}{|q|\xi} \right). \quad (65)$$

This expression generalizes that for the angular velocity at which a straight vortex at the center of a thin disk-shape condensate becomes metastable [9], including the corrections of order  $\alpha^{-1}$  and  $\beta^{-1}$ .

### C. Dynamics of a vortex in a cigar-shape condensate $R_z \gg R_\perp$ : Investigation of unstable modes

In the opposite limit  $\alpha, \beta \ll 1$ , the unstable-mode solution of Eqs. (55) and (56) corresponds to exponential growth of the vortex displacement as a function of  $z$ . Such a solution is possible in 3D because the condensate is bounded along the  $z$  axis.

For simplicity, consider an axisymmetric trap, so that  $\alpha = \beta$ . In this case, we have only one equation because one can seek a solution in the form  $x(z) = y(z)$ :

$$\tilde{\omega}x = \frac{2(\alpha z x' - x)}{(1 - z^2)} - \alpha x'' + \tilde{\Omega}x, \quad (66)$$

In the limit  $\alpha \ll 1$  Eq. (66) has the following approximate solution

$$x = y = \varepsilon e^{|z|/\alpha}, \quad (67)$$

$$\tilde{\omega} = -\frac{1}{\alpha} + \tilde{\Omega}. \quad (68)$$

The approximate solution (67) has a nonanalytic behavior at  $z = 0$ , where a thin boundary layer appears. The actual solution differs from (67) in a small vicinity of  $z = 0$  and represents a smooth crossover from the region  $z < 0$  into the region  $z > 0$ . Equation (68) yields the metastable angular velocity  $\Omega_m$  in an elongated cigar-shape condensate

$$\Omega_m = \frac{|q|\hbar(\omega_x^2 + \omega_y^2)}{8\mu} \frac{R_z^2}{R_\perp^2} \ln \left( \frac{R_\perp}{|q|\xi} \right). \quad (69)$$

In contrast to Eq. (65) for a flattened condensate, this expression becomes very large for highly elongated trap. Consequently, it is significantly more difficult to stabilize a vortex in a cigar-shape condensate than in one with a disk shape.

#### D. Numerical results for 3D

We have used Eq. (66) to evaluate the eigenvalues and eigenfunctions for an axisymmetric trap ( $\alpha = \beta$ ). A finite trap rotation produces only a shift of eigenvalues by  $\tilde{\Omega}$ , so we can set  $\tilde{\Omega} = 0$ . In addition, solutions of Eq. (66) can be classified as even or odd functions of  $z$ . One can enumerate the solutions by the number  $m$  of times that the vortex line crosses  $z$  axis,  $m = 0, 1, 2, \dots$ . The lowest (most negative) eigenvalue corresponds to  $m = 0$ .

In Fig. 2 we plot the angular velocity of the vortex precession  $\tilde{\omega}$  as a function of the trap anisotropy  $\alpha = R_\perp^2/R_z^2$  for  $m = 0, 1, 2$ . In appropriate limits, the numerical solution  $\tilde{\omega}_0$  coincides with those found analytically:  $\tilde{\omega}_0 \approx -3 - \frac{1}{5}\alpha$  for  $\alpha \geq 1$ , and  $\tilde{\omega}_0 \approx -1/\alpha$  for  $\alpha \ll 1$ . The next two solutions  $\tilde{\omega}_1$  and  $\tilde{\omega}_2$  are proportional to  $\alpha$  for large  $\alpha$  and diverge like  $-1/\alpha$  for small  $\alpha$ . If  $\alpha > 1$  only one mode has a negative frequency (namely  $\tilde{\omega}_0$ ). If  $\frac{1}{3} < \alpha < 1$  there are 2 such normal modes; if  $\frac{1}{6} < \alpha < \frac{1}{3}$  there are 3 modes, *etc.* (these numerical results coincide with those found analytically).

The more elongated the trap, the larger the number of modes with negative frequencies (see also [44]). This conclusion represents one of our main findings. For a disk-shape condensate, the angular velocity  $\Omega_m$  for the onset of metastability is smaller than the thermodynamic critical angular velocity  $\Omega_c$ , with  $\Omega_m = \frac{3}{5}\Omega_c$  [9]. The situation is completely different for a cigar-shape condensate with  $\alpha = R_\perp^2/R_z^2 < 0.26$ , because  $\Omega_m$  then becomes larger than  $\Omega_c$ . For comparison, Fig. 2 includes the line  $\tilde{\omega} = -\tilde{\Omega}_c = -5$ .

In Fig. 3 we plot the shape of the vortex line for the lowest (unstable) normal mode ( $m = 0$ ) for different values of trap anisotropy  $\alpha$ . The function  $x(z)$  is an even function of  $z$  without nodes and  $\varepsilon = x(z = 0)$ . In Fig. 4 and 5 we plot the shape of the vortex line for normal modes with one and two nodes for different values of trap anisotropy  $\alpha$ . In Fig. 4  $x_{\max} = |x(z = R_z)|$ .

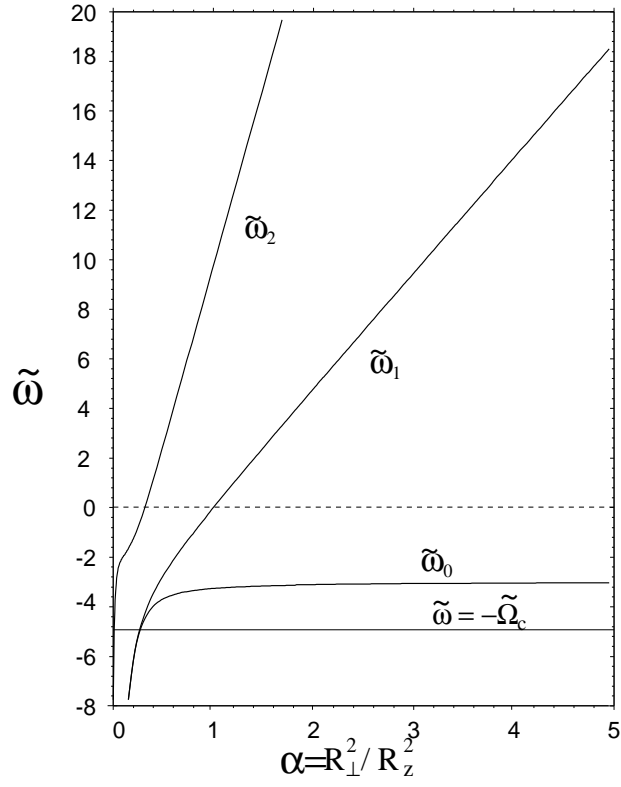


Fig. 2. Dimensionless frequencies  $\tilde{\omega}$  of the first three normal modes of the vortex as a function of the trap anisotropy  $\alpha = R_{\perp}^2/R_z^2$ . The lower horizontal line represents the dimensionless thermodynamic critical angular velocity.

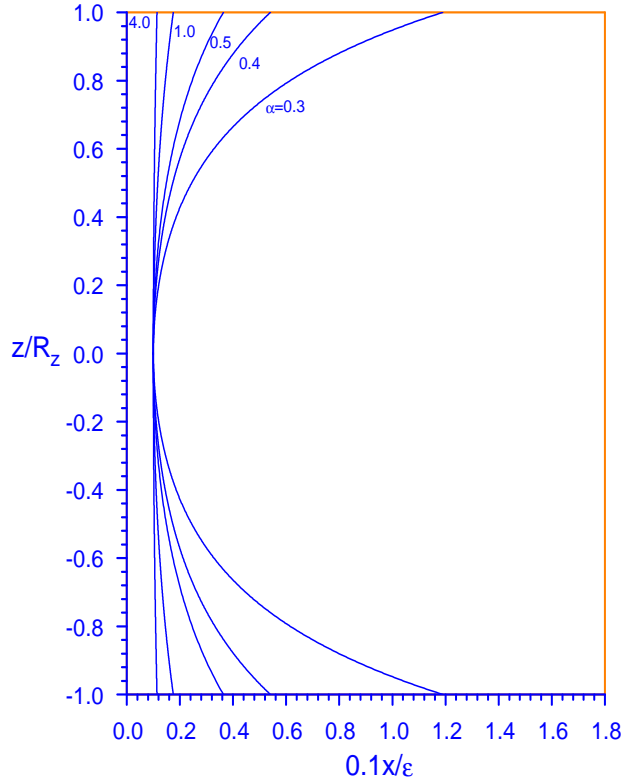


Fig. 3. Shape of the vortex line for the normal mode with the lowest frequency (the most unstable mode) for different values of the trap anisotropy  $\alpha$ .

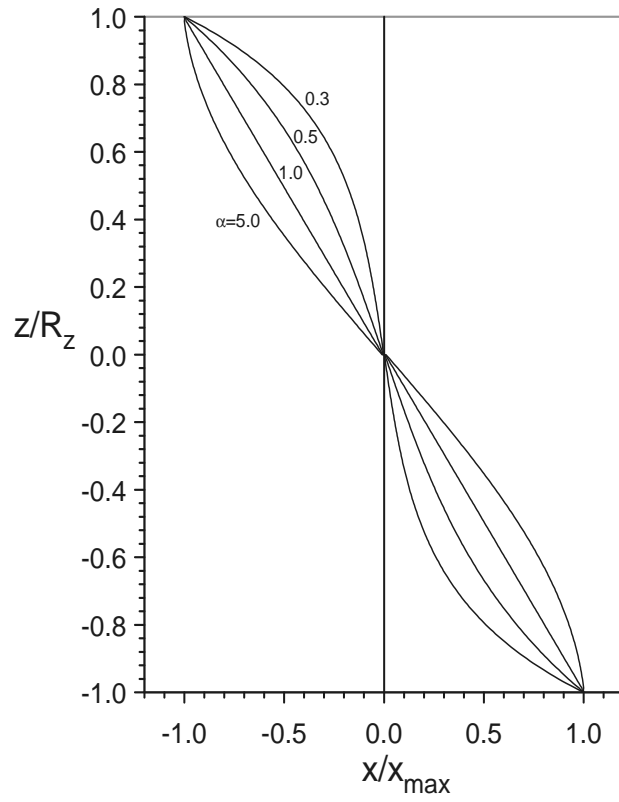


Fig. 4. Shape of the vortex line for the first odd normal mode for different  $\alpha$ .

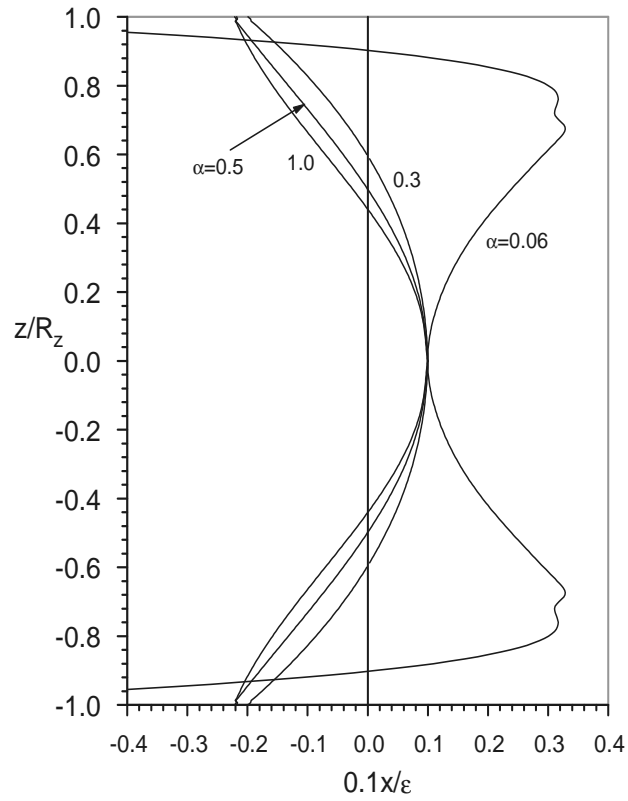


Fig. 5. Shape of the vortex line for the second even normal mode for different  $\alpha$ .

## V. NORMAL MODES OF A VORTEX WITH IMAGINARY FREQUENCIES FOR A NONAXISYMMETRIC 3D CONDENSATE

For an axisymmetric trap all small-amplitude normal modes have real frequencies. For a nonaxisymmetric trap ( $\alpha \neq \beta$ ), however, Eqs. (55), and (56) can have solutions with imaginary frequencies (in certain regimes of trap anisotropy). As an example, we recall that a spherical trap has a special normal mode with  $m = 1$  and  $\tilde{\omega} = 0$ . Let us now consider a nearly spherical trap (this geometry is relevant to the JILA experiments [45])

$$|\alpha - 1| \ll 1, \quad |\beta - 1| \ll 1.$$

One can rewrite Eqs. (55) and (56) as follows:

$$\tilde{\omega}(1 - z^2) \begin{pmatrix} x \\ y \end{pmatrix} = \hat{H}_0 \begin{pmatrix} x \\ y \end{pmatrix} + \hat{V} \begin{pmatrix} x \\ y \end{pmatrix}, \quad (70)$$

where

$$\hat{H}_0 = -\{2 + \partial_z[(1 - z^2)\partial_z]\} \begin{pmatrix} 0 & 1 \\ 1 & 0 \end{pmatrix},$$

$$\hat{V} = -\partial_z[(1 - z^2)\partial_z] \begin{pmatrix} 0 & \beta - 1 \\ \alpha - 1 & 0 \end{pmatrix} + (1 - z^2)\tilde{\Omega} \begin{pmatrix} 0 & 1 \\ 1 & 0 \end{pmatrix},$$

and  $\hat{V}$  is a small perturbation.

The unperturbed equation corresponds to the equation for the normal modes of a vortex in a spherical nonrotating trap and, therefore, all eigenfrequencies of the unperturbed equation are real. The eigenvalue  $\tilde{\omega} = 0$  of the unperturbed equation is degenerate, and there are two solutions that correspond to  $\tilde{\omega} = 0$ :

$$\begin{pmatrix} x_1 \\ y_1 \end{pmatrix} = \begin{pmatrix} z \\ 0 \end{pmatrix}, \quad \begin{pmatrix} x_2 \\ y_2 \end{pmatrix} = \begin{pmatrix} 0 \\ z \end{pmatrix}. \quad (71)$$

The eigenfunctions of  $\hat{H}_0$  are Legendre polynomials, and these eigenfunctions form a complete basis. Therefore, one can apply the usual perturbation theory to solve Eq. (70). The matrix elements are given by:

$$V_{11} = V_{22} = 0,$$

$$V_{12} = \frac{4}{3} \left( \beta - 1 + \frac{1}{5}\tilde{\Omega} \right),$$

$$V_{21} = \frac{4}{3} \left( \alpha - 1 + \frac{1}{5}\tilde{\Omega} \right).$$

To first order in the perturbation, the eigenfrequencies have the form

$$\tilde{\omega} = \pm \frac{\sqrt{V_{12}V_{21}}}{\int_{-1}^1 (1 - z^2)z^2 dz} = \pm 5 \sqrt{\left( \alpha - 1 + \frac{1}{5}\tilde{\Omega} \right) \left( \beta - 1 + \frac{1}{5}\tilde{\Omega} \right)}. \quad (72)$$

If, for example,  $\alpha < 1 < \beta$  (namely  $R_x < R_z < R_y$ ), then the solutions have imaginary frequencies for  $\tilde{\Omega} < 5(1 - \alpha)$ :

$$\tilde{\omega} = \pm i\gamma, \quad \gamma = 5 \sqrt{\left( 1 - \alpha - \frac{1}{5}\tilde{\Omega} \right) \left( \beta - 1 + \frac{1}{5}\tilde{\Omega} \right)} > 0. \quad (73)$$

Here, the imaginary frequency means a vortex line oriented along the  $z$  axis (which is the intermediate principal axis in our example) corresponds to an unstable equilibrium. In contrast, a vortex line oriented along the other principal axes is stable. If the angular velocity of the trap rotation increases, however, then the solution (72) becomes real for  $\tilde{\Omega} > 5(1 - \alpha)$  and the vortex line along the  $z$  axis becomes stable because of the rotation.

It is straightforward to consider a general anisotropic trap (not necessarily close to a spherical shape). The result is the following: if the parameters  $\alpha$  and  $\beta$  satisfy the inequality:

$$\alpha < \frac{2}{n(n+1)} < \beta, \quad (74)$$

where  $n$  is a non-negative integer, then there is a normal-mode solution with imaginary frequency that corresponds to the  $n$ th Legendre polynomial. Moreover, if

$$\alpha < \frac{2}{n(n+1)} < \frac{2}{m(m+1)} < \beta, \quad (75)$$

then there are  $(n - m + 1)$  solutions with imaginary frequencies. Increasing the external trap rotation sequentially eliminates such solutions.

## VI. MOTION OF A STRAIGHT VORTEX LINE IN A SLIGHTLY NONSPHERICAL 3D CONDENSATE

In the previous sections, we studied the motion of the vortex line for small displacements of the vortex from equilibrium position (normal modes). In this section we solve the general nonlinear equation of the vortex dynamics (38) for a slightly nonspherical trap. This problem is directly related to a recent JILA experiment involving the evolution of an initially straight vortex line in a nearly spherical condensate [45]. In practice, the trap slightly deviates from the spherical shape ( $R_x \neq R_y \neq R_z$ ).

For a strictly spherical trap, Eq. (38) has a solution representing a motionless straight vortex line ( $\hat{t} \parallel \nabla V_{\text{tr}}$ ) that passes through the center of the trap, with the shape

$$x = \gamma_x s, \quad y = \gamma_y s, \quad z = \gamma_z s. \quad (76)$$

Here  $s$  is the length measured along the vortex line starting from the trap center and  $\gamma_x, \gamma_y, \gamma_z$  are the direction cosines of the angles between the vortex line and the principal axes  $x, y, z$  [so that  $\gamma_x^2 + \gamma_y^2 + \gamma_z^2 = 1$ ,  $\hat{t} = (\gamma_x, \gamma_y, \gamma_z)$ ]. For a slightly anisotropic trap, however, the solution has approximately the same form as (76), but the coefficients  $\gamma_x, \gamma_y, \gamma_z$  become time-dependent. To find a solution to first order in the trap anisotropy, one can omit the curvature of the vortex line and put  $k = 0$  in (38). Also we should use the vortex-free condensate density  $|\Psi_{TF}|^2$  and take  $R_{\perp}$  to be equal to the value for a spherical trap. Using the standard perturbation theory, we obtain the following equations for the coefficients  $\gamma_x, \gamma_y, \gamma_z$  (here, we assume that there is no trap rotation):

$$\begin{pmatrix} \dot{\gamma}_x \\ \dot{\gamma}_y \\ \dot{\gamma}_z \end{pmatrix} = \frac{q\hbar}{2\mu} \frac{\int_{-R}^R s^2 ds}{\int_{-R}^R s^2 (1 - \frac{s^2}{R^2}) ds} \ln \left( \frac{R}{|q|\xi} \right) \begin{pmatrix} \gamma_y \gamma_z (\omega_z^2 - \omega_y^2) \\ \gamma_x \gamma_z (\omega_x^2 - \omega_z^2) \\ \gamma_x \gamma_y (\omega_y^2 - \omega_x^2) \end{pmatrix}, \quad (77)$$

or, evaluating the integrals,

$$\dot{\gamma}_x = \frac{5q\hbar}{4\mu} \ln \left( \frac{R}{|q|\xi} \right) (\omega_z^2 - \omega_y^2) \gamma_y \gamma_z, \quad (78)$$

$$\dot{\gamma}_y = \frac{5q\hbar}{4\mu} \ln \left( \frac{R}{|q|\xi} \right) (\omega_x^2 - \omega_z^2) \gamma_x \gamma_z, \quad (79)$$

$$\dot{\gamma}_z = \frac{5q\hbar}{4\mu} \ln \left( \frac{R}{|q|\xi} \right) (\omega_y^2 - \omega_x^2) \gamma_x \gamma_y. \quad (80)$$

Equations of this type are known in classical mechanics as Euler's equations of rigid-body motion; they describe the evolution of the angular velocity of free motion of a body with different principal moments of inertia as seen in the body-fixed frame [46]. Equations (78)-(80) have the following integrals of motion:

$$\gamma_x^2 + \gamma_y^2 + \gamma_z^2 = 1, \quad (81)$$

$$\omega_x^2 \gamma_x^2 + \omega_y^2 \gamma_y^2 + \omega_z^2 \gamma_z^2 = \text{const.} \quad (82)$$

That is, the ends of the straight vortex move along trajectories that correspond to the intersection of a sphere and an ellipsoid with principal axes proportional to  $R_x$ ,  $R_y$ ,  $R_z$ . In fact, Eq. (82) is the equation of energy conservation during the vortex motion.

In the particular case of an axisymmetric trap (for example,  $\omega_x = \omega_y = \omega_\perp$ ), Eqs. (78)-(80) have the following solution

$$\gamma_z = \gamma_z(0) = \text{const}, \quad (83)$$

$$\gamma_x = \gamma_x(0) \cos(\omega t) + \gamma_y(0) \sin(\omega t), \quad (84)$$

$$\gamma_y = \gamma_y(0) \cos(\omega t) - \gamma_x(0) \sin(\omega t), \quad (85)$$

where

$$\omega = \frac{5q\hbar(\omega_z^2 - \omega_\perp^2)}{4\mu} \gamma_z(0) \ln \left( \frac{R}{|q|\xi} \right) = \frac{5q\hbar}{2M} \left( \frac{1}{R_z^2} - \frac{1}{R_\perp^2} \right) \gamma_z(0) \ln \left( \frac{R}{|q|\xi} \right), \quad (86)$$

and  $[\gamma_x(0), \gamma_y(0), \gamma_z(0)]$  fixes the initial orientation of the vortex line. The line precesses around the  $z$  axis (the axis of symmetry) at a fixed angle of inclination with respect to the  $z$  axis. The frequency of this precession depends on the inclination and vanishes if the vortex line is perpendicular to the  $z$  axis with  $\gamma_z(0) = 0$ .

We now consider a general nonaxisymmetric trap. To be specific, we assume that  $\omega_x > \omega_y > \omega_z$  and introduce new scaled functions

$$\delta_x = \frac{5q\hbar}{4\mu} \ln \left( \frac{R}{|q|\xi} \right) \sqrt{(\omega_x^2 - \omega_z^2)(\omega_x^2 - \omega_y^2)} \gamma_x, \quad (87)$$

$$\delta_y = \frac{5q\hbar}{4\mu} \ln \left( \frac{R}{|q|\xi} \right) \sqrt{(\omega_y^2 - \omega_z^2)(\omega_x^2 - \omega_y^2)} \gamma_y, \quad (88)$$

$$\delta_z = \frac{5q\hbar}{4\mu} \ln \left( \frac{R}{|q|\xi} \right) \sqrt{(\omega_y^2 - \omega_z^2)(\omega_x^2 - \omega_z^2)} \gamma_z. \quad (89)$$

Then one can rewrite Eqs. (78)-(80) as follows:

$$\dot{\delta}_x = -\delta_y \delta_z, \quad (90)$$

$$\dot{\delta}_y = \delta_x \delta_z, \quad (91)$$

$$\dot{\delta}_z = -\delta_x \delta_y. \quad (92)$$

These equations have the following property: if  $\delta_x$ ,  $\delta_y$ ,  $\delta_z$  is a solution of these equations, then if we change sign of any two functions (for example,  $\delta_x \rightarrow -\delta_x$ ,  $\delta_y \rightarrow -\delta_y$ ,  $\delta_z \rightarrow \delta_z$ ), we obtain another solution. This property can serve to construct solutions that satisfy specific initial conditions. Equations (90)-(92) have three stationary solutions. Two of them (the vortex line parallel to the  $x$  or  $z$  axis) correspond to a stable equilibrium, while the third solution (the vortex parallel to the  $y$  axis) is an unstable equilibrium.

If  $|\delta_x(0)| < |\delta_z(0)|$ , the vortex line oscillates around  $z$  axis (this is one of the equilibrium orientations), and one can express the solution of Eqs. (90)-(92) in terms of Jacobian elliptic functions as follows:

$$\delta_x = \sqrt{\delta_x^2(0) + \delta_y^2(0)} \operatorname{cn} \left( \sqrt{\delta_z^2(0) + \delta_y^2(0)} t + C, k \right), \quad (93)$$

$$\delta_y = \pm \sqrt{\delta_x^2(0) + \delta_y^2(0)} \operatorname{sn} \left( \sqrt{\delta_z^2(0) + \delta_y^2(0)} t + C, k \right), \quad (94)$$

$$\delta_z = \pm \sqrt{\delta_z^2(0) + \delta_y^2(0)} \operatorname{dn} \left( \sqrt{\delta_z^2(0) + \delta_y^2(0)} t + C, k \right), \quad (95)$$

where the modulus  $k = \sqrt{\delta_x^2(0) + \delta_y^2(0)} / \sqrt{\delta_z^2(0) + \delta_y^2(0)}$  is less than one, and  $C$  is a constant that must be chosen to satisfy the initial conditions. The solution is a periodic function of time with the period

$$T = \frac{4}{\sqrt{\delta_z^2(0) + \delta_y^2(0)}} \int_0^{\pi/2} \frac{d\varphi}{\sqrt{1 - k^2 \sin^2 \varphi}} = \frac{4}{\sqrt{\delta_z^2(0) + \delta_y^2(0)}} K(k), \quad (96)$$

where  $K(k)$  is the complete elliptical integral of the first kind. The solution (93)-(95) represents a superposition of a nonuniform circular motion in a plane perpendicular to the  $z$  axis and oscillations along the  $z$  axis:  $\delta_z$  oscillates within the following segment:

$$\sqrt{\delta_z^2(0) - \delta_x^2(0)} \leq |\delta_z| \leq \sqrt{\delta_z^2(0) + \delta_y^2(0)} \quad (97)$$

If  $|\delta_x(0)| > |\delta_z(0)|$  (the modulus  $k$  is greater than one), the vortex line oscillates around  $x$  axis. In this case one can use reciprocal modulus transformation ( $k \cdot \operatorname{sn}(u, k) = \operatorname{sn}(ku, 1/k)$ ,  $\operatorname{cn}(u, k) = \operatorname{dn}(ku, 1/k)$ ,  $\operatorname{dn}(u, k) = \operatorname{cn}(ku, 1/k)$ ) and rewrite the solution (93)-(95) as follows

$$\delta_x = \pm \sqrt{\delta_x^2(0) + \delta_y^2(0)} \operatorname{dn} \left( \sqrt{\delta_x^2(0) + \delta_y^2(0)} t + \tilde{C}, 1/k \right), \quad (98)$$

$$\delta_y = \pm \sqrt{\delta_z^2(0) + \delta_y^2(0)} \operatorname{sn} \left( \sqrt{\delta_x^2(0) + \delta_y^2(0)} t + \tilde{C}, 1/k \right), \quad (99)$$

$$\delta_z = \sqrt{\delta_z^2(0) + \delta_y^2(0)} \operatorname{cn} \left( \sqrt{\delta_x^2(0) + \delta_y^2(0)} t + \tilde{C}, 1/k \right). \quad (100)$$

The solution is a periodic function of time with the period

$$T = \frac{4}{\sqrt{\delta_z^2(0) + \delta_y^2(0)}} \int_0^{\pi/2} \frac{d\varphi}{\sqrt{k^2 - \sin^2 \varphi}} = \frac{4}{\sqrt{\delta_x^2(0) + \delta_y^2(0)}} K(1/k). \quad (101)$$

If  $|\delta_x(0)| = |\delta_z(0)|$  ( $k = 1$ ), the solution reduces to

$$\delta_x = \pm \delta_z = \frac{\sqrt{\delta_x^2(0) + \delta_y^2(0)}}{\cosh \left( \sqrt{\delta_x^2(0) + \delta_y^2(0)} t + C \right)}, \quad (102)$$

$$\delta_y = \pm \sqrt{\delta_x^2(0) + \delta_y^2(0)} \tanh \left( \sqrt{\delta_x^2(0) + \delta_y^2(0)} t + C \right); \quad (103)$$

during the motion, the vortex remains on a plane through the  $y$  axis, oriented along  $\delta_x = \pm \delta_z$  (see Fig. 6); it eventually lines up along the  $y$  axis (which is a direction of unstable equilibrium for the geometry  $\omega_x > \omega_y > \omega_z$  that we are considering).

Finally, one can rewrite these solutions directly in terms of the parameters  $\gamma_x, \gamma_y, \gamma_z$  that describe the orientation of the vortex line. For example, instead of (93)-(96), we have

$$\gamma_x = \sqrt{\gamma_x^2(0) + \frac{(\omega_y^2 - \omega_z^2)}{(\omega_x^2 - \omega_z^2)} \gamma_y^2(0)} \cdot \operatorname{cn}(\omega t + C, k), \quad (104)$$

$$\gamma_y = \pm \sqrt{\gamma_y^2(0) + \frac{(\omega_x^2 - \omega_z^2)}{(\omega_y^2 - \omega_z^2)} \gamma_y^2(0)} \cdot \operatorname{sn}(\omega t + C, k), \quad (105)$$



$$\gamma_z = \pm \sqrt{\gamma_z^2(0) + \frac{(\omega_x^2 - \omega_y^2)}{(\omega_x^2 - \omega_z^2)} \gamma_y^2(0)} \cdot \text{dn}(\omega t + C, k), \quad (106)$$

where

$$k = \sqrt{\frac{(\omega_x^2 - \omega_y^2) [(\omega_x^2 - \omega_z^2) \gamma_x^2(0) + (\omega_y^2 - \omega_z^2) \gamma_y^2(0)]}{(\omega_y^2 - \omega_z^2) [(\omega_x^2 - \omega_z^2) \gamma_z^2(0) + (\omega_x^2 - \omega_y^2) \gamma_y^2(0)]}}, \quad (107)$$

$$\begin{aligned} \omega &= \frac{5q\hbar \sqrt{\omega_y^2 - \omega_z^2}}{4\mu} \sqrt{(\omega_x^2 - \omega_z^2) \gamma_z^2(0) + (\omega_x^2 - \omega_y^2) \gamma_y^2(0)} \ln \left( \frac{R}{|q|\xi} \right) \\ &= \frac{5q\hbar}{2M} \sqrt{\frac{1}{R_y^2} - \frac{1}{R_z^2}} \sqrt{\left( \frac{1}{R_x^2} - \frac{1}{R_z^2} \right) \gamma_z^2(0) + \left( \frac{1}{R_x^2} - \frac{1}{R_y^2} \right) \gamma_y^2(0)} \ln \left( \frac{R}{|q|\xi} \right). \end{aligned} \quad (108)$$

The period of the motion is given by

$$T = \frac{4}{\omega} \int_0^{\pi/2} \frac{d\varphi}{\sqrt{1 - k^2 \sin^2 \varphi}} = \frac{4}{\omega} K(k). \quad (109)$$

For a nonaxisymmetric trap we plot trajectories of the end of the vortex line in Fig. 6. The plot corresponds to the geometry  $R_x < R_y < R_z$ . There are two stable orientations (along the  $x$  and  $z$  axes) and one unstable (along the  $y$  axis). The shape of the trajectories strongly depends on the initial orientation of the vortex.

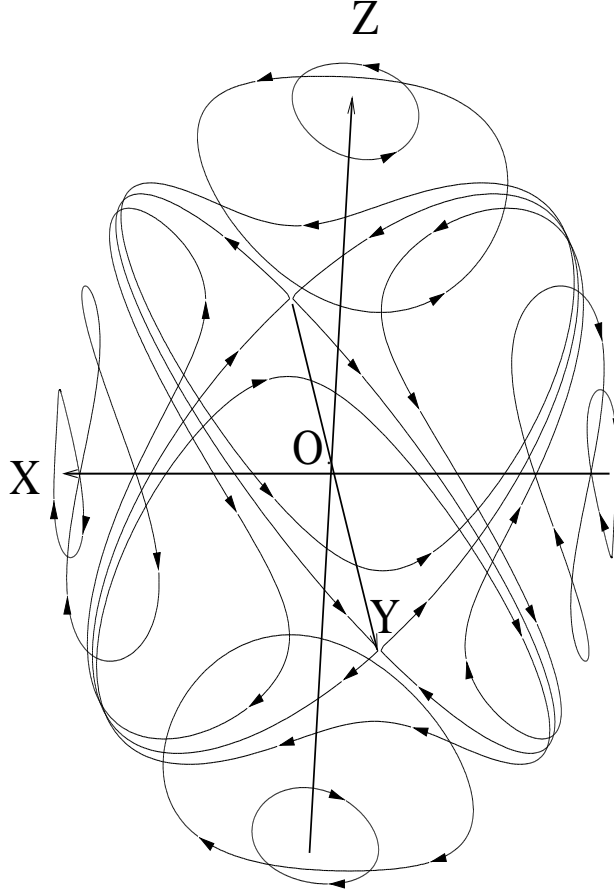


Fig. 6. Typical trajectories of the end of a straight vortex line (that passes through the condensate center) during its motion in a slightly nonspherical trap with  $R_x < R_y < R_z$ .

For an axisymmetric trap, we have  $\omega_x = \omega_y$  so that  $k = 0$ . Then, using the properties  $\text{sn}(z, 0) = \sin z$ ,  $\text{cn}(z, 0) = \cos z$ ,  $\text{dn}(z, 0) = 1$ , we can reproduce formulas (83)-(86).

Because the motion is periodic, one can anticipate one or more revivals of the vortex image in the recent JILA experiments. The revival time depends on the orientation of the vortex with respect to the symmetry axes and the deviations from sphericity. Recently, such revivals of the vortex image (as well as vortex precession [25]) was seen by the JILA group, and their results agree quantitatively with our theory [45]. One should note that our analytical results for the normal-mode frequencies are valid with the logarithmic accuracy, namely when  $\ln(R/|q|\xi) \gg 1$ . It is, however, straightforward to go beyond logarithmic accuracy and obtain the numerical correction to the logarithm (see Ref. [35]). This correction modifies our formulas for the normal-mode frequencies as follows: instead of  $\ln(R/|q|\xi)$ , one should use  $\ln(R/|q|\xi) + 0.675 = \ln(1.96R/|q|\xi)$ . In the JILA experiments,  $\ln(R/\xi) \approx 3.5$ , and the inclusion of the correction improves the quantitative agreement with the experimental observations.

## VII. CONCLUSIONS

In this paper, we consider the dynamics of a vortex line in 2D and 3D condensates in the TF limit. We took into account the nonuniform nature of the system (namely the trap potential), the vortex curvature and a possible trap rotation. We derived a general equation of vortex dynamics and investigated various normal modes of the vortex line. For an axisymmetric trap, all eigenvalues are real and the motion of the vortex line can be represented as a superposition of planar normal modes with different frequencies. In a 2D condensate, the normal modes are degenerate, and, as a result, a superposition of planar waves can produce helical waves. In 3D, there is no such degeneracy and there is no simple analog of the helical waves.

An externally applied trap rotation  $\Omega$  shifts the normal-mode frequencies and makes the vortex locally stable for sufficiently large  $\Omega$ . For a cigar-shape condensate, the vortex curvature has a significant effect on the frequency of the most unstable normal mode (that with the most negative frequency), and additional modes with (less) negative frequencies appear. As a result, it is more difficult to stabilize central vortex in a cigar-shape condensate than in a disc-shape one.

Normal modes with imaginary frequencies can exist for a nonaxisymmetric condensate (both in 2D and 3D). This means that the corresponding equilibrium orientation of the vortex is unstable. As an example of the solution of the general nonlinear problem of vortex dynamics, we considered the motion of a straight vortex line in a slightly nonspherical condensate. The vortex line changes its orientation in space at a rate proportional to the trap anisotropy.

## ACKNOWLEDGMENTS

This work was supported in part by the National Science Foundation, Grant No. DMR 99-71518, and by Stanford University (A.A.S.). We are grateful to B. Anderson, J. Anglin, E. Cornell and D. Feder for valuable correspondence and discussions. This work benefitted from our participation in recent workshops at the Lorentz Center, Leiden, The Netherlands and at ECT\* European Centre for Theoretical Studies in Nuclear Physics and Related Areas, Trento, Italy; we thank H. Stoof and S. Stringari for organizing these workshops and for their hospitality.

- 
- [1] M. H. Anderson *et al.*, *Science* **269**, 198 (1995).
  - [2] C. C. Bradley *et al.*, *Phys. Rev. Lett.* **75**, 1687 (1995).
  - [3] K. B. Davis *et al.*, *Phys. Rev. Lett.* **75**, 3969 (1995).
  - [4] B. Jackson, J. F. McCann, and C. S. Adams, *Phys. Rev. Lett.* **80**, 3903 (1998).
  - [5] R. Dum *et al.*, *Phys. Rev. Lett.* **80**, 2972 (1998).
  - [6] K. P. Marzlin, W. Zhang, and E. M. Wright, *Phys. Rev. Lett.* **79**, 4728 (1997).
  - [7] G. Baym and C. J. Pethick, *Phys. Rev. Lett.* **76**, 6 (1996).
  - [8] F. Dalfovo and S. Stringari, *Phys. Rev. A* **53**, 2477 (1996).
  - [9] A. A. Svidzinsky and A. L. Fetter, *Phys. Rev. Lett.* **84**, 5919 (2000).
  - [10] D. L. Feder, C. W. Clark, and B. I. Schneider, *Phys. Rev. Lett.* **82**, 4956 (1999).
  - [11] B. Jackson, J. F. McCann, and C. S. Adams, *Phys. Rev. Lett.* **80**, 3903 (1998).

- [12] E. L. Bolda and D. F. Walls, Phys. Lett. A **246**, 32 (1998).
- [13] T. Winiecki, J. F. McCann and C. S. Adams, Phys. Rev. Lett. **82**, 5186 (1999).
- [14] J. R. Anglin and W. H. Zurek, Phys. Rev. Lett. **83**, 1707 (1999).
- [15] R. J. Marshall *et al.*, Phys. Rev. A **59**, 2085 (1999).
- [16] P. D. Drummond and J. F. Corney, Phys. Rev. A **60**, R2661 (1999).
- [17] L. Dobrek *et al.*, Phys. Rev. A **60**, R3381 (1999).
- [18] B. Jackson, J. F. McCann, and C. S. Adams, Phys. Rev. A **60**, 4882 (1999).
- [19] M. Olshani, and M. Naraschewski, e-print cond-mat/9811314.
- [20] J. Ruostekoski, B. Kneer and W. P. Schleich, e-print cond-mat/9908095.
- [21] M. R. Matthews *et al.*, Phys. Rev. Lett. **83**, 2498 (1999).
- [22] K. W. Madison *et al.*, Phys. Rev. Lett. **84**, 806 (2000).
- [23] K. W. Madison *et al.*, e-print cond-mat/0004037.
- [24] F. Chevy, K. W. Madison and J. Dalibard, e-print cond-mat/0005221.
- [25] B. P. Anderson *et al.*, e-print cond-mat/0005368.
- [26] L. P. Pitaevskii, Zh. Eksp. Teor. Fiz. **40**, 646 (1961) [Sov. Phys. JETP **13**, 451 (1961)].
- [27] A. A. Svidzinsky and A. L. Fetter, Phys. Rev. A **58**, 3168 (1998).
- [28] R. J. Donnelly, *Quantized Vortices in Helium II* (Cambridge University Press, Cambridge, 1991).
- [29] F. Lund, Phys. Lett. A **159**, 245 (1991).
- [30] S. Rica and E. Tirapegui, Physica D **61**, 246 (1992).
- [31] S. Rica and E. Tirapegui, Phys. Rev. Lett. **64**, 878 (1990).
- [32] J. Koplik and H. Levine, Phys. Rev. Lett. **71**, 1375 (1993).
- [33] J. Koplik and H. Levine, Phys. Rev. Lett. **76**, 4745 (1996).
- [34] Yu. Kivshar *et al.*, Optics Comm. **152**, 198 (1998).
- [35] B. Y. Rubinstein and L. M. Pismen, Physica D **78**, 1 (1994).
- [36] E. Lundh, and P. Ao, Phys. Rev. A **61**, 063612 (2000).
- [37] L. M. Pismen and J. Rubinstein, Physica D **47**, 353 (1991).
- [38] R. J. Dodd *et al.*, Phys. Rev. A **56**, 587 (1997).
- [39] M. Linn and A. L. Fetter, Phys. Rev. A **60**, 4910 (1999); **61**, 063603 (2000).
- [40] B. Jackson, J. F. McCann, and C. S. Adams, Phys. Rev. A **61**, 013603 (2000).
- [41] Y. Castin and R. Dum, Eur. Phys. J. D **7**, 399 (1999).
- [42] P. O. Fedichev and G. V. Shlyapnikov, Phys. Rev. A **60**, R1779 (1999).
- [43] A. A. Svidzinsky and A. L. Fetter, Physica B **284-288**, 21 (2000).
- [44] J. J. García-Ripoll and V. M. Pérez-García, Phys. Rev. A **60**, 4864 (1999).
- [45] E. A. Cornell, private communication.
- [46] See, for example, D. Kleppner and R. Kolenkow, *An Introduction to Mechanics* (McGraw-Hill, New York, 1973), Sec. 7.7.